Title

The effects of dilution and mixed layer depth on deliberate ocean iron fertilization: 1-D simulations of the southern ocean iron experiment (SOFeX)

Journal

Journal of Marine Systems, 71(1-2)

ISSN

0924-7963

Authors

Krishnamurthy, Aparna
Moore, J Keith
Doney, Scott C

Publication Date

2008-05-01

DOI

10.1016/j.jmarsys.2007.07.002

Available online at www.sciencedirect.com
ScienceDirect
Journal of Marine Systems 71 (2008) 112–130
JOURNAL OF MARINE SYSTEMS
www.elsevier.com/locate/jmarsys

The effects of dilution and mixed layer depth on deliberate ocean iron fertilization: 1-D simulations of the southern ocean iron experiment (SOFeX)

Aparna Krishnamurthy [a,*], J. Keith Moore [a], Scott C. Doney [b]

[a] Earth System Science Department, University of California, Irvine, CA 92697, USA
[b] Department of Marine Chemistry and Geochemistry, Woods Hole Oceanographic Institution, Woods Hole, MA 02543, USA

Received 14 December 2006; received in revised form 6 July 2007; accepted 12 July 2007
Available online 26 July 2007

Abstract

To better understand the role of iron in driving marine ecosystems, the Southern Ocean Iron Experiment (SOFeX) fertilized two surface water patches with iron north and south of the Antarctic Polar Front Zone (APFZ). Using 1-D coupled biological–physical simulations, we examine the biogeochemical dynamics that occurred both inside and outside of the fertilized patches during and shortly after the SOFeX field campaign. We focus, in particular, on three main issues governing the biological response to deliberate iron fertilization: the interaction among phytoplankton, light, macronutrient and iron limitation; dilution and lateral mixing between the fertilized patch and external, unfertilized waters; and the effect of varying mixed layer depth on the light field. At the patch south of the APFZ, sensitivity simulations with no dilution results in the maximum bloom magnitude, whereas dilution with external water extends the development of the north patch bloom by relieving silicon limitation. In model sensitivity studies for both sites, maximum chlorophyll concentration and dissolved inorganic carbon depletion inside the fertilized patches are inversely related to mixed layer depth, similar to the patterns observed across a number of iron fertilization field experiments. Our results suggest that Southern Ocean phytoplankton blooms resulting from natural or deliberate iron fertilization will tend to become iron-light co-limited unless the mixed layer depth is quite shallow.

Keywords: SOFeX; Southern Ocean; HNLC; Marine ecosystem model; Nutrient limitation; Light limitation; Mixed layer depth; Phytoplankton community; Iron fertilization

1. Introduction

Southern Ocean surface waters contain high levels of macronutrients but relatively modest levels of chlorophyll, in most regions. Theories postulated to explain these high nutrient, low chlorophyll (HNLC) waters include deep mixing along with light limitation (Mitchell et al., 1991; Nelson and Smith, 1991), plankton community structure and strong grazing pressure (Brown and Landry, 2001), and iron limitation (Martin, 1990). Multiple factors impact the seasonal cycle of phytoplankton growth in these regions (Boyd et al., 1999; Abbott et al., 2000; Fennel et al., 2003; Smith and Lancelot, 2004), with light limitation dominating during early spring followed by iron limitation after the onset of water column stratification. During austral summer diatom growth may become silicon limited, particularly in subantarctic waters. Deep mixed layers can

* Corresponding author. Tel.: +1 949 824 2314; fax: +1 949 824 3874.
E-mail address: aparnak@uci.edu (A. Krishnamurthy).

0924-7963/$ - see front matter © 2007 Elsevier B.V. All rights reserved.
doi:10.1016/j.jmarsys.2007.07.002

also result in co-limitation by iron and light, as the phytoplankton cellular requirement for iron increases under light stress (Sunda and Huntsman, 1997; Boyd, 2002).

Among the factors mentioned above, it is now well established that in HNLC areas the limitation of micronutrient iron largely prevents the full consumption of macronutrients by phytoplankton. This has been demonstrated for Southern Ocean HNLC waters in several mesoscale iron fertilization experiments, where artificial additions of iron resulted in increased chlorophyll, primary productivity and phytoplankton biomass (Boyd et al., 2000; Smetacek 2001; Coale et al., 2004).

The Southern Ocean Iron Experiment (SOFeX) was conducted during austral summer of 2002 in the Pacific sector of the Southern Ocean (Coale et al., 2004). It involved fertilizing two patches, one north of the Antarctic Polar Front Zone (APFZ) characterized in austral spring by low-silicate, high nitrate waters (North Patch) and one south of the APFZ characterized by high-silicate, high-nitrate waters (South Patch). These two regions were selected such that the hydrography, nutrients and the biogeochemical provinces could represent larger areas of the Southern Ocean. Apart from testing the iron hypothesis, the experiment was also intended to test whether low silicate ($Si(OH)_4$) conditions north of the APFZ would diminish the fertilization response because of diatom Si limitation.

The North Patch was created on 12th January, 2002 at 56.23° S, 172° W, and the South Patch was created on 24th January, 2002 at 66.45° S, 171.8° W. Successive iron additions were done by injecting acidified iron sulfate into the ship's wake such that mixed layer iron concentrations were raised to 1.2 nM, 1.2 nM, 1.5 nM at the North Patch, and four additions were done at the South Patch such that iron concentrations were 0.7 nM after each addition. Sulfur hexafluoride (SF_6) was added along with iron during the first infusion to track the patches. The enriched patches were studied by three research vessels, *R/V* Revelle, *R/V* Melville and *R/V* Polar Star for a period of 40 and 28 days for the north and south sites, respectively (supplemental material, Coale et al., 2004). Particulate organic carbon (POC), temperature and salinity in the upper 1000 m were measured using three free-profiling Lagrangian Carbon Explorers at 55° S and one at 66° S deployed from the *R/V* Revelle (Bishop et al., 2004). These Explorers also estimated carbon export at 100 m using an optically derived carbon flux index.

Satellite remote sensing indicates that the unfertilized waters in the region of the SOFeX South Patch sometimes exhibit a natural seasonal chlorophyll bloom, while natural blooms are absent for the North Patch region (Moore and Doney, 2006). During the period of SOFeX, background surface chlorophyll levels at the South Patch were low compared to climatological conditions at that site and to nearby locations to the east and west of the study location. Moore and Doney (2006) hypothesize that these differences could have arisen from variable iron supply from melting sea ice and icebergs along with increased stratification at the southern site. Their study concluded that there was a delay in the melting of sea-ice during the growing season of 2001–2002 compared to other years. This led to a delay in the naturally occurring modest spring bloom from December to January–February in this region.

Our purpose here is to examine, using 1-D coupled biological–physical numerical simulations, the biogeochemical dynamics that occurred both inside and outside of the fertilized patches during and shortly after the SOFeX field campaign. We focus, in particular, on three main issues governing the biological response to iron fertilization: the interaction among phytoplankton, light, macronutrient and iron limitation; the effects of dilution and lateral mixing between the fertilized and unfertilized waters; and variations in mixed layer depth and mixed layer light field.

Like all deliberate ocean fertilization studies, the SOFeX fertilized patches were finite in horizontal extent and underwent lateral mixing with the surrounding unfertilized waters. The North Patch was located at the subantarctic frontal zone, a region of fronts that elongated the patch from a square into a long, thin filament (~ 7 km $\times$ 340 km) by day 38. The South Patch extended more slowly in all directions (Coale et al., 2004; Moore and Doney, 2006). Dilution rates can be estimated in two ways. One is to find the amount of physical strain of tracer filament when the patch stretches. During the Southern Ocean iron release experiment (SOIREE), for example, the dispersal of the tracer due to dilution was estimated by locally resolving the tracer flow into pure strain and rotation (Abraham et al., 2000). The extent of this stretching can be obtained also from satellite ocean color observations. During the SOFeX, a dilution rate of 0.11 per day at the North Patch and 0.086 per day at the South Patch was obtained using this technique (Coale et al., 2004). A second way is to estimate dilution rates by calculating the loss of SF_6, accounting for outgassing. Dilution rate estimates during the SOFeX using this method were 0.1 per day at the North Patch and 0.03 to 0.07 per day at the South Patch (Coale et al., 2004). There was a variation in SF_6 derived estimates because of inhomonogeneities within the patch and analytical variability. Coale et al. (2004) used dilution rates 0.08 per day for South Patch and 0.11 per day for North Patch as a best estimate. We adopted these values of dilution in our baseline simulations.

Lateral mixing brings macronutrients into the fertilized waters as well as diluting the products of the bloom (Boyd et al., 2000; Abraham et al., 2000). For our model simulations, a constant dilution rate was applied at each SOFeX site. Through a suite of sensitivity experiments where we adjust dilution from zero to a reasonable upper bound, we find that mixing due to dilution was particularly important at the low-silicate North Patch where the supply of Si $(OH)_4$ rich waters into the fertilized patch (Hiscock and Millero, 2005) relieves Si limitation and extends the bloom.

The biological response to iron fertilization is also modulated by mixed layer depth (MLD), a proxy for the average light level for phytoplankton growth in the surface layer. In the Southern Ocean, shallow MLDs and the associated elevated light levels most favorable for phytoplankton growth occur during the austral summer months (Campbell and Aarup, 1989). During this period, mixed layer depth is sensitive to wind driven vertical mixing. In order to qualitatively access the role of changing light levels on nutrient uptake, biological production and export, we conducted a second suite of sensitivity experiments varying wind forcing and thus MLD.

The remainder of the paper is constructed as follows. In Section 2, we describe the coupled 1-D biological–physical simulations using the KPP model (Large et al., 1994) and the marine ecosystem model of Moore et al. (2002, 2004) used to simulate biogeochemical dynamics inside and outside the fertilized surface water patches at both SOFeX sites. In Section 3.1, we evaluate the 1-D simulations by comparing model estimates of primary production, nutrients, chlorophyll, POC and its export, biogenic silica, and silicification rate with those obtained during the experiment. We also discuss how nutrient and light-limitation modulates the growth of various phytoplankton groups in the simulations. Sensitivity experiments on lateral dilution (Section 3.2) and mixed layer depth (Section 3.3) provide qualitative estimates of the effects of these physical dynamics on biological response during deliberate iron fertilization in the Southern Ocean region, with implications for the natural system as well. Carbon and iron budgets (Section 3.4) during the 60-day simulations provide a summary of organic carbon and iron partitioned among the various pools. The paper concludes with a summary and discussion section (Section 4).

2. Methods

2.1. Biogeochemical elemental cycling model

We used a one-dimensional implementation of the marine Biogeochemical Elemental Cycling model (hereafter called BEC), described in Moore et al. (2004). The 1-D column model has 150, 1 m thick horizontal levels that include the euphotic zone and shallow aphotic zones. The model includes phytoplankton growth limitation by multiple nutrients (N, P, Fe, and Si) and multiple phytoplankton classes (pico/nano-plankton, diatoms, diazotrophs, and coccolithophores). Depending upon nutrient availability and physical forcing, the model is robust enough to shift the phytoplankton community structure from diatoms, with high production rates and high export, to a small phytoplankton dominated, low-production, low-export system.

Diatoms and small phytoplankton (representing the nano and pico-sized species) are included in the model. Diazotrophs have been modeled based on information on *Trichodesmium* spp. (Moore et al., 2002). Biomass of diazotrophs was always negligible in the simulations for this region and they are not discussed further here. Coccolithophores are parameterized as a function of small phytoplankton production, and their biomass changes as a function of nutrient limitation, temperature and bloom conditions with a constraint that calcification rate not exceed a maximum of 40% of the small phytoplankton group primary production. Photoadaptation is calculated as a variable phytoplankton ratio of chlorophyll to nitrogen based on Geider et al. (1998). Phytoplankton growth is parameterized to include balanced growth and multiple potentially limiting nutrients. Growth rate can be limited by nitrogen (nitrate, ammonia), phosphorus, iron, silicon (for diatoms), and/or ambient light. As the light and nutrient levels change, the model incorporates variable elemental ratios for C/Fe, C/Si, and C/Chlorophyll. The losses of the four phytoplankton groups occurs via respiration/natural mortality, zooplankton grazing and phytoplankton aggregation. Detailed description of the model is available in Moore et al., (2002, 2004).

2.2. Model implementation

Surface forcing values including wind stress, atmospheric pressure, and net heat and fresh water fluxes were obtained from NCEP reanalysis data (Kalnay et al., 1996), and daily mean surface photosynthetically available radiation (PAR) data was obtained from SeaWiFS (McClain et al., 1998, 2004). PAR within each layer was calculated using an attenuation coefficient, $kPAR = 0.03\ (m^{-1}\ (mg\ Chl)^{-1}\ m^3) * Chl + 0.04\ m^{-1}$). Climatological dust/iron deposition from atmosphere was obtained from Luo et al. (2003). The model was run at each site without fertilization to define the "out of patch" temporal history. For the fertilized patch cases, these results were used to simulate dilution from surrounding waters using the Coale

et al. (2004) estimates of dilution of 0.08 per day at the South Patch and 0.11 per day at the North Patch. This horizontal dilution of in patch and out of patch waters was applied daily at all depths. This is a necessary simplification of the complex 3D circulation and mixing that occurred in situ. It is meant only to capture to 1st order the effects of lateral patch dilution. Surface boundary layer dynamics were simulated by using the non-local turbulent mixing scheme described by Large et al. (1994). This utilized wind stress, net heat flux, and net fresh water input to predict the development of surface boundary layer and vertical profiles of temperature, salinity and other biological scalars (Doney, 1996).

Mean mixed layer depths were 35 m and ~40 m at the North Patch in the model and observations, respectively, and 32 m and 35–40 m at the South Patch in the model and observations, respectively. On a few days in our simulations, the mixed layer shoaled, reducing the mean mixed layer depth values; otherwise simulated values were close to observed values. NCEP wind speeds at the South Patch were reduced by 15% in the baseline simulation to better match the observed mixed layer depth.

Total small phytoplankton, diatom, diazotroph and zooplankton biomass at both patches were set to values obtained after an initial (unfertilized) spin-up simulation. Surface nitrate, phosphate, and silicate concentrations were set similar to those prior to the fertilization experiment at both the North and South Patches. The observational dissolved iron data for outside the fertilized patches were limited and also as low as 0.06 nM (Kenneth Coale per. communications), significantly lower than the biological half-saturation coefficients used in the ecosystem model. Thus, they were not sufficient in initial simulations for the model to reproduce the unfertilized patch conditions. Rather than adjust the model coefficients, we set the initial iron profiles at the South Patch to a uniform value of 0.15 nM to a depth of 50 m increasing linearly to 0.3 nM at 150 m and at the North Patch from 0.1 nM to a depth of 50 m increasing linearly to 0.2 nM at 150 m. These values were obtained for this region from the global simulations of the model (Moore et al., 2004).

Model outputs of nutrients, chlorophyll, POC and C/Chl ratios were averaged over the upper 20 m at both patches and were compared with mixed layer observations from SOFeX. Integrated values of biogenic silica were obtained for the upper 50 m of the water column, and sinking POC export was calculated at 50 m. Primary production and silicification were integrated over the entire 150 m of water column. These were compared with experimental observations at corresponding depths.

Sensitivity studies were performed at both the North and South Patches to estimate the effect of varying dilution rates and mixed layer depths. Scenarios were simulated with no dilution, and 0.5 and 1.5 times the Coale et al. (2004) estimates. Using these dilution rates, lateral dilution of all biogeochemical tracers between fertilized and unfertilized simulations was computed daily over all depths in our 150 m domain. Mixed layer depth sensitivity simulations were conducted by varying the baseline adjusted NCEP wind forcing by factors of 0.7, 1.3 and 1.6. The simulations with modified mixed layer depths and dilution rates had the same initial biogeochemical profiles as the standard simulations.

2.3. Ecosystem parameter changes

The ecosystem model parameters used by Moore et al. (2004) were optimized for the global domain. It is not surprising, then, that application to a particular region may require some parameter adjustments. Parameters were modified so that the simulations provided a better match to the data for the South Patch, where field observations provided better constraints; this modified parameter set was used for both patches. The original Moore et al. (2004) parameter set resulted in a South Patch diatom bloom that was much smaller than the observed bloom. Several parameters were tuned to better simulate the observations. The maximum zooplankton grazing rate when feeding on diatoms was decreased from 2.07 to 1.7 per day. The coefficient used in the quadratic terms in aggregation mortality for small phytoplankton and diatoms was also lowered from 0.009 to 0.006 (decreasing aggregation losses). The half saturation constant (Ks) for silica uptake at the North Patch was estimated at 0.63 μM by Brzezinski et al. (2005) during the SOFeX. We changed from our standard value of 1.0 μM to 0.63 μM

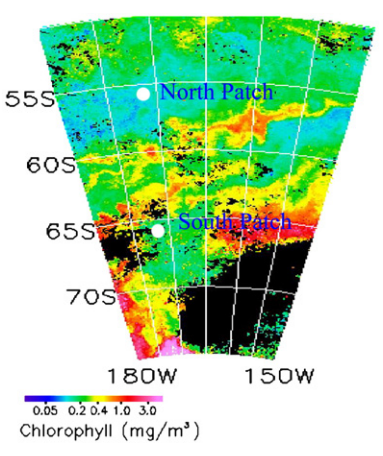

Fig. 1. Geographical map of the region where the SOFeX fertilizations occurred (white dots) over a map of mean chlorophyll concentration for January 2001 from the SeaWiFS sensor.

only for North Patch (silicate concentrations were always high and non-limiting at the South Patch).

The initial slope of the irradiance vs. production curve, α (mmol C m^2/mg Chl W day), was reduced from 0.3 to 0.25 at both patches. This value is close to that observed during SOFeX (0.12 and 0.22) in the unfertilized and fertilized surface waters respectively (Hiscock, 2004). The mean value of α obtained from other cruises in the Southern Ocean region were 0.23 (Dehairs et al., 2000), 0.19 (Gervais et al., 2002), 0.2 (Helbling et al., 1995), and 0.21 (Hiscock, 2004). The maximum cellular chlorophyll to nitrogen ratios were modified from 2.3 and 3.0, to 2.25 and 4.5 mg Chl/mmol N for small phytoplankton and diatoms, respectively. These changes brought the model into better agreement with the culture observations of Geider et al. (1998) for diatom vs. non-diatoms, giving the diatoms an enhanced ability to adapt to low light levels.

The temperature dependent growth rate factor, q_{10}, was reduced from a doubling to a multiple of 1.65 and 1.75 for every 10° C rise of temperature at the South and North Patch respectively. This improved the timing of the blooms, but it does not necessarily mean that the modified q_{10} value applies to this region as the temperature range of each simulation is too small to evaluate q_{10} robustly; a similar effect would have resulted from increasing the model maximum growth and grazing rates at the reference temperature.

The partitioning of organic carbon into sinking POC export and DOC were modified such that the simulated

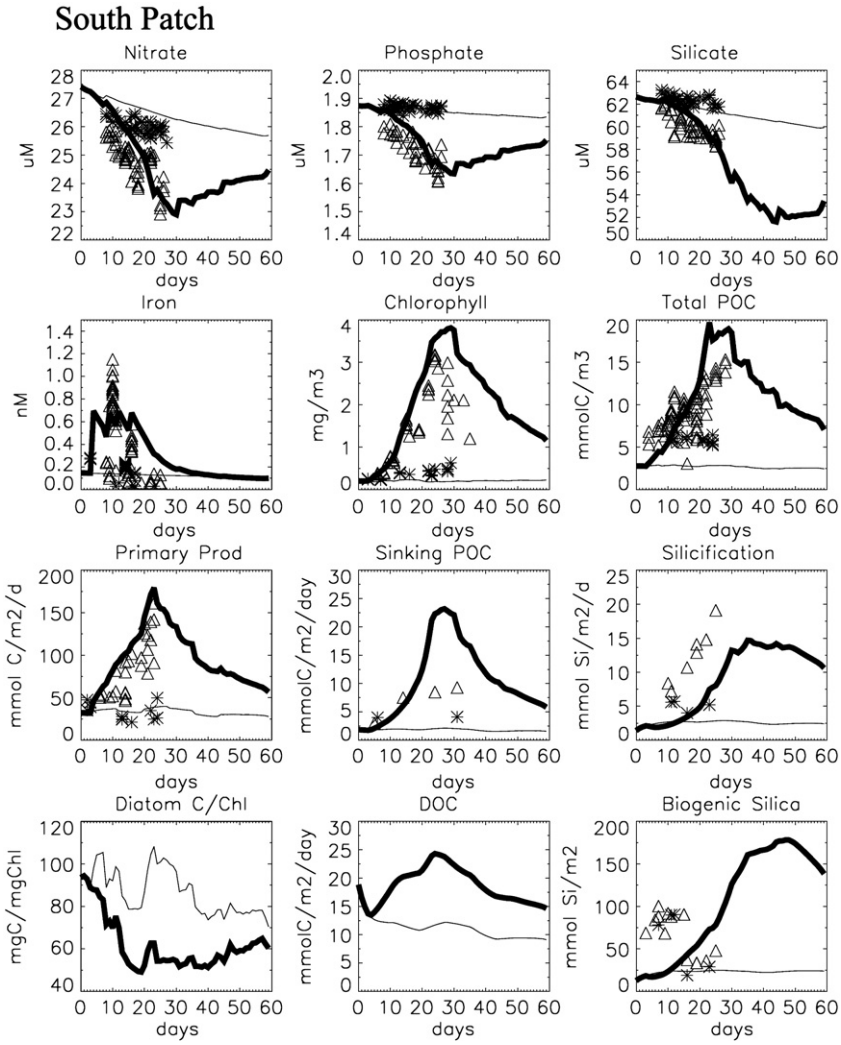

Fig. 2. Results obtained from simulations for the South Patch. The simulated results of unfertilized waters and iron fertilized patch are depicted by light and dark lines, respectively. The experimental observations from SOFeX for outside and inside the iron fertilized patch are depicted by asterisks and triangles, respectively.

export of sinking POC was closer to observational estimates during the SOFeX. This change decreased the fraction of grazed material going to sinking POM and increased the fraction going to DOM by 50% for both the diatom and small phytoplankton groups.

3. Results

3.1. Model-data comparisons

Model simulations for North Patch started on January 7th, 2002 and ended 60 days later on March 7th, 2002. The geographical location (in white dots) where the simulations were performed is shown in Fig. 1. Note the low (<0.2 mg/m^3) ambient chlorophyll concentrations in the region. The last field observations at the North Patch were made on February 22nd, 2002. The South Patch simulations started on January 21st, 2002 and ended 60 days later on March 21st, 2002. The last field observations at the South Patch were made on February 21st, 2002. In our series of model-data time series plots, the thin line represents simulated unfertilized, outside patch conditions and the thick line represents fertilized, inside patch simulations. The asterisk and triangle represent the unfertilized and fertilized patch observations, respectively.

The temporal trends in nutrient drawdown at the South Patch compared well with the observations reported by Hiscock and Millero (2005) (Fig. 2). Note the strong drawdown and export of silicic acid in the

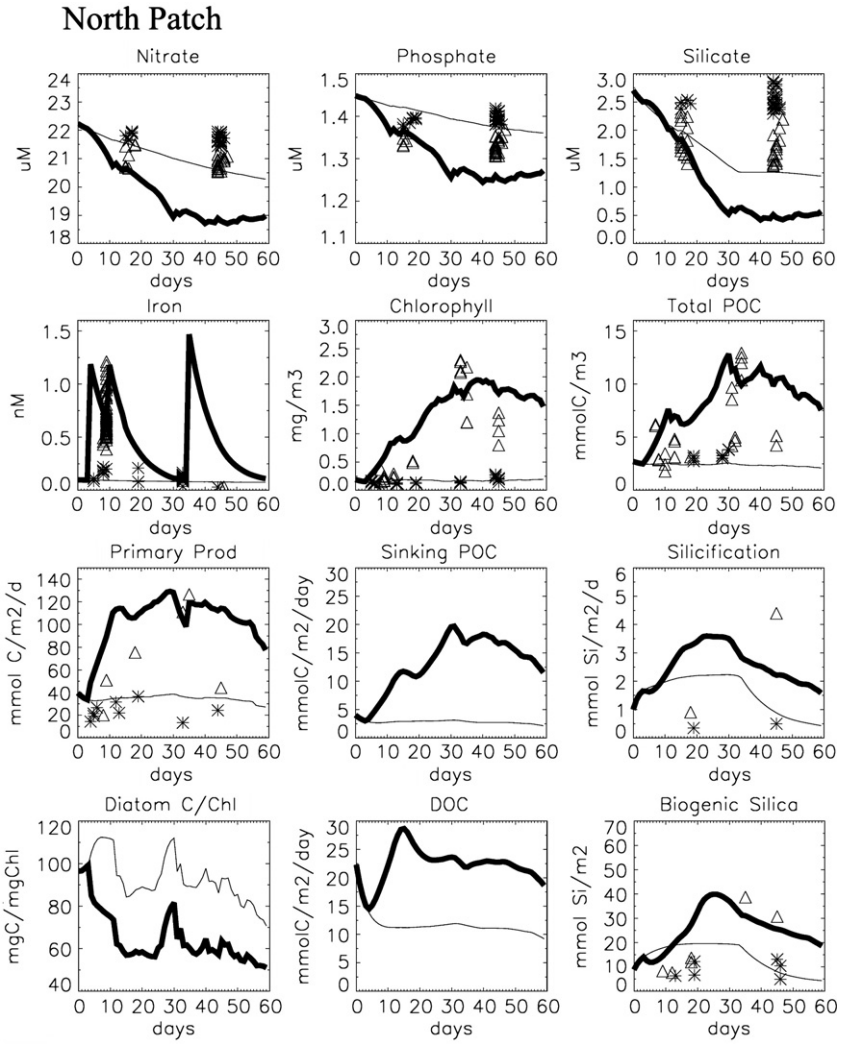

Fig. 3. Results obtained from simulations for the North Patch. The simulated results of unfertilized waters and iron fertilized patch are depicted by light and dark lines, respectively. The experimental observations from SOFeX for outside and inside the iron fertilized patch are depicted by asterisks and triangles, respectively.

Table 1
Model-observation comparisons between the difference in concentrations of biogeochemical tracers averaged over the mixed layer depth in the fertilized and unfertilized surface waters on day 28 (North Patch) and day 30 (South Patch) (observations from Table 1 of Coale et al., 2004)

	North Patch		South Patch	
	Observations	Model	Observations	Model
Chlorophyll (mg/m^3)	2.6	1.6	4	2.8
TCO_2 depletion (mmol C/m^3)	15±2	13.0	16±6	22.0
Nitrate depletion (μM)	−2±0.2	−1.9	−1.9±0.7	−3.2
Silicic acid depletion(μM)	−1.5	−0.7	−4	−6.2
POC accumulation (mmol C/m^3)	8.5±0.8	8.9	11±3	11.9
Biogenic silica (mmol Si/m^3)	1.2	0.5	4.2	4.1

simulations following the end of the field campaign. Seasonal diatom blooms are characteristic for this region of the Southern Ocean, with preferential drawdown and export of Si accounting for the observed high nitrate, low silicic acid conditions at the North Patch. At the unfertilized surface waters (thin line), simulated chlorophyll and total POC are underestimated whereas primary productivity is within the range of the observational dataset. Simulated values of chlorophyll and primary productivity inside the fertilized patch correspond well with the high-end observations (those closer to the patch center, Fig. 2). Peak values of simulated total POC are somewhat overestimated (Coale et al., 2004; POC data from Mark Altabet (UM, Dartmouth) & Craig Hunter (MLML), and primary productivity from Lance et al., 2007).

At the North Patch, simulated phosphate, nitrate and silicate in the fertilized surface waters were lower than the observations (Hiscock and Millero, 2005) (Fig. 3). The observational data for the macronutrient concentrations show very little variability at both unfertilized and fertilized surface waters suggesting dominance of nutrient entrainment from ambient waters. Model predictions of chlorophyll and total POC were in general agreement with

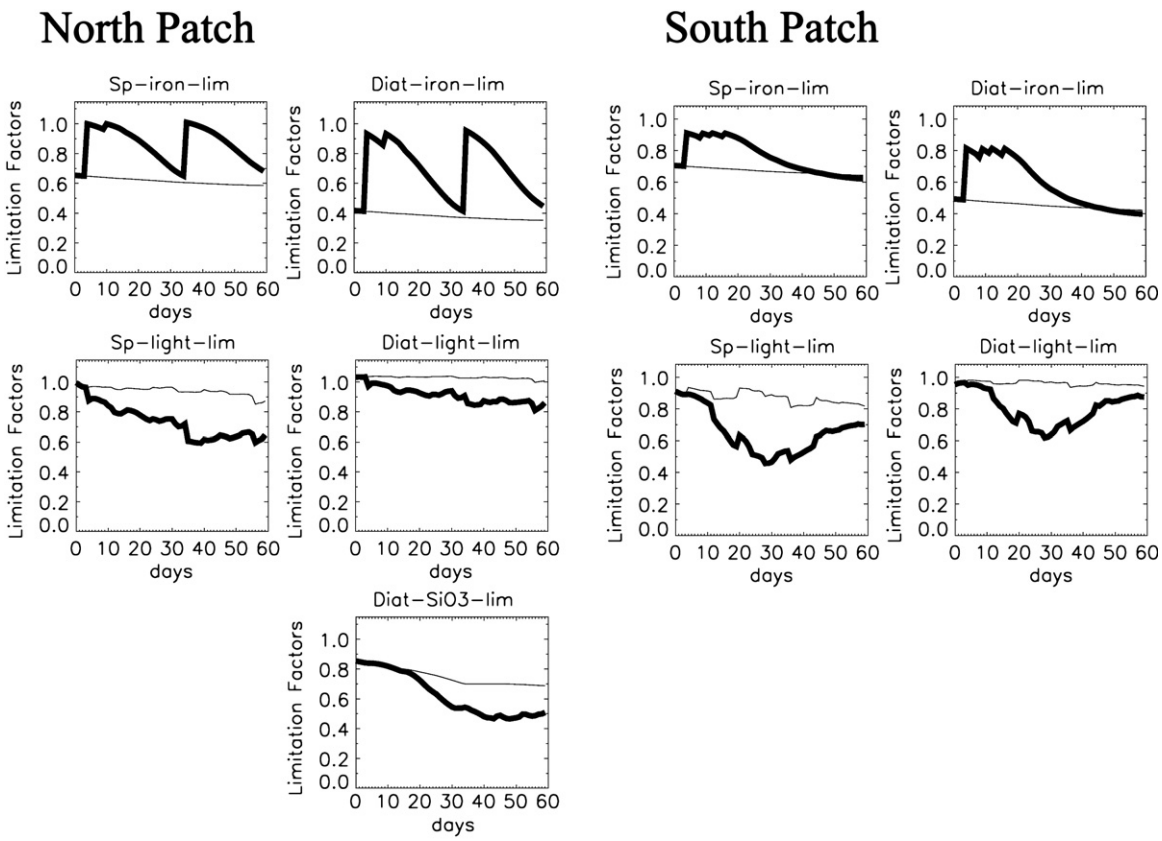

Fig. 4. Mixed layer depth averages of the growth-limitation-factors (*y*-axis, factors multiplied by the maximum growth rate to give relative reduction in growth rate) for the small phytoplankton (Fe and light) and for the diatoms (Fe, Si, and light) at each patch site. Model results outside and inside the iron fertilized patches are depicted by light and dark lines, respectively.

the observations in the unfertilized simulation (Coale et al., 2004; POC data from Altabet & Hunter). Simulated chlorophyll and total POC in the fertilized patch also correspond well with the observed maximum values. The observed maximum integrated primary productivity over the euphotic zone compares well with that obtained from simulations for both the control and fertilized patches (Lance et al., 2007), though the model bloom develops somewhat earlier than that in the data for the fertilized case.

The South Patch POC export was measured at 25 m, 50 m and 100 m with thorium isotopes; it increased from 2–5 mmol C/m^2/day in unfertilized waters to 2–11 mmol C/m^2/day in the fertilized patch (Buesseler et al., 2005). Our simulation overestimates sinking POC export inside the South Patch compared to these observations (Fig. 2). The North Patch sinking POC export in the fertilized waters was estimated bio-optically from profiling floats as described in Bishop et al. (2004). Using two indirect POC flux measurement techniques, they obtained values of 20 to 190 mmol C/m^2 and 760 to 1170 mmol C/m^2 between days 39 and 55 of the experiment. This wide range brackets our simulation at the North Patch.

During the SOFeX, biogenic silica and silica production rates were estimated by Brzezinski et al. (2005). At the South Patch, the model lags the observed rise in silica production in the fertilized case by about a

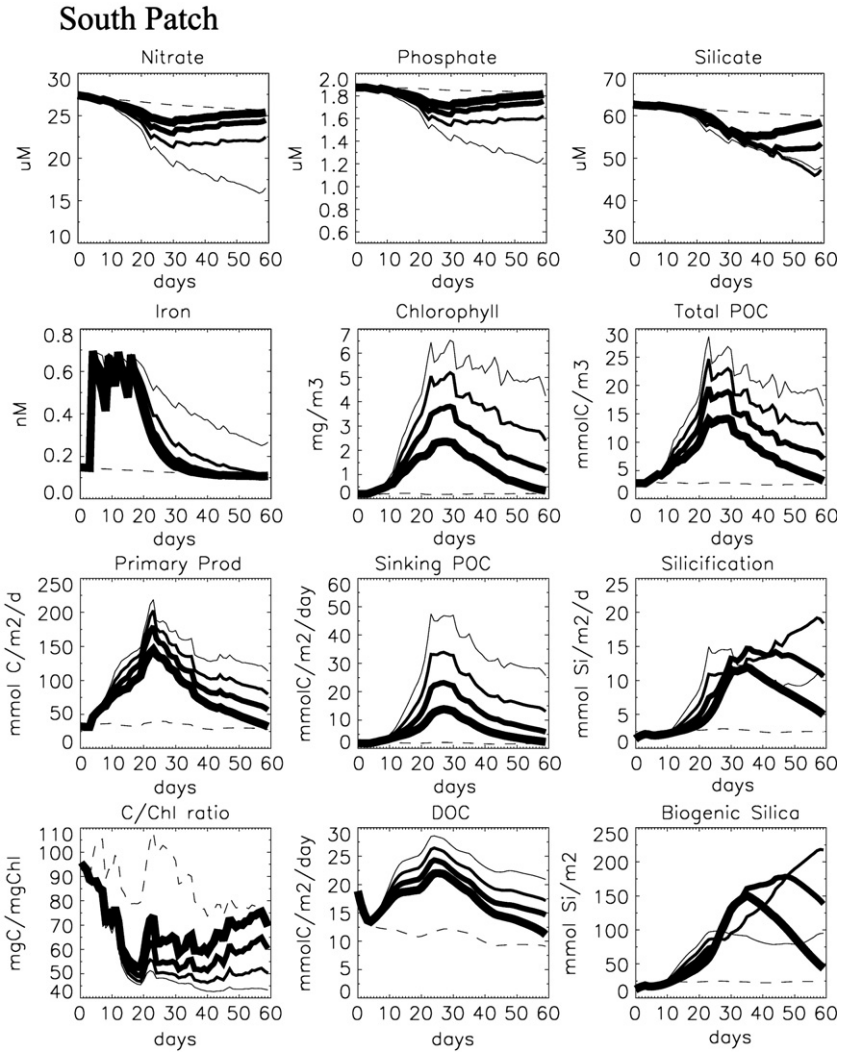

Fig. 5. Results obtained from simulations for the iron fertilized South Patch with varying dilution rates. Solid lines with increasing thickness depict the simulations with no dilution, 0.5 * Coale et al. (2004) dilution, Coale et al. (2004) dilution, and 1.5 * Coale et al. (2004) dilution, respectively. Dashed line depicts the simulated unfertilized surface waters.

week (Fig. 2). Silica production at the North Patch did not compare well with the limited observations. At the South Patch, the simulated biogenic silica values are within the maximum observational estimates of biogenic silica (for <day 30). After this period, there are no observational estimates for making comparisons. At the North Patch, the simulated diatom bloom occurs too early; elevated rates and build-up of biogenic silica in the observations only appear after day 30 following the third iron injection (Fig. 3). Brzezinski et al. (2005) stated that the biogenic silica values obtained from the sampling regions were diluted by surrounding waters. This resulted in the lowering of biogenic silica at the South and North Patches.

The South Patch bloom was terminated in our simulation when iron returned to background levels shortly after the field campaign ended. At the North Patch chlorophyll and POC remain elevated throughout our simulations, at somewhat higher than observed concentrations. As the bloom developed the simulated diatom carbon to chlorophyll ratios decreased at both the patches because when the diatoms become light stressed they synthesize more chlorophyll per unit carbon (Figs. 2 and 3). This light stress was always stronger for the inside patch simulations compared to that at the outside patch simulations, due to self-shading by the bloom. The integrated DOC production at both patches was also estimated from simulations, but field

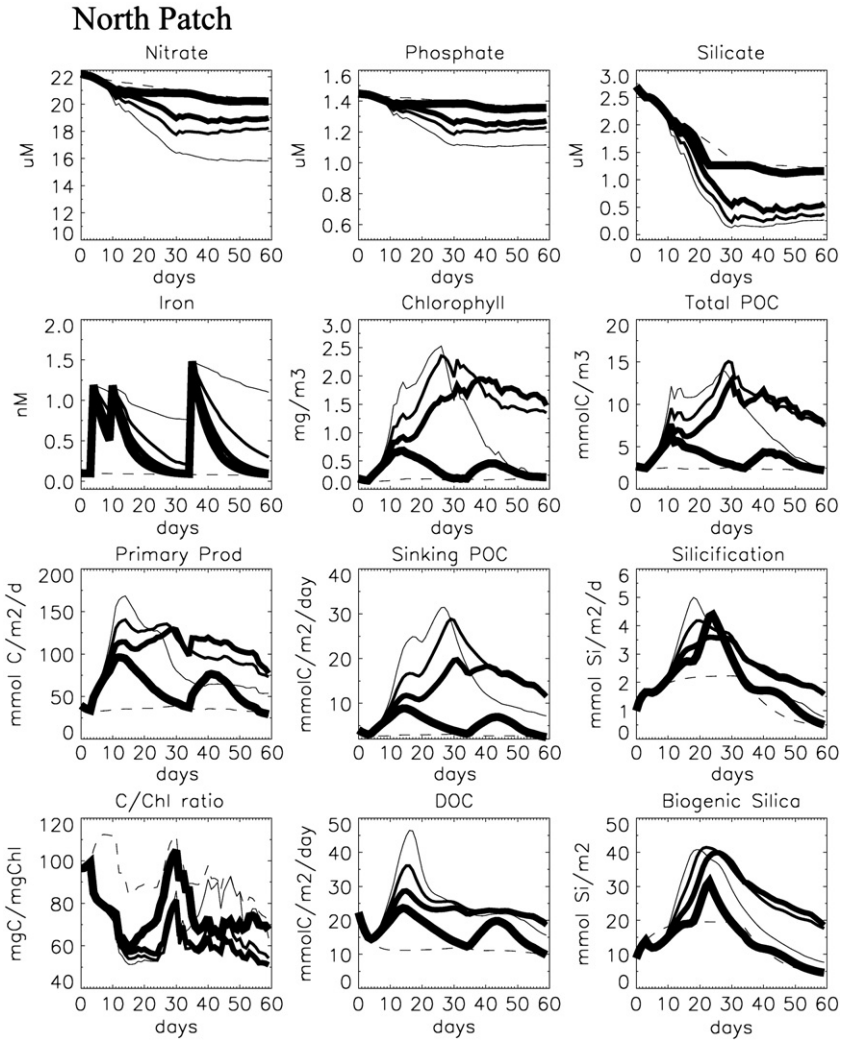

Fig. 6. Results obtained from simulations for the iron fertilized North Patch with varying dilution rates. Solid lines with increasing thickness depict the simulations with no dilution, 0.5 * Coale et al. (2004) dilution, Coale et al. (2004) dilution, and 1.5 * Coale et al. (2004) dilution, respectively. Dashed line depicts the simulated unfertilized surface waters.

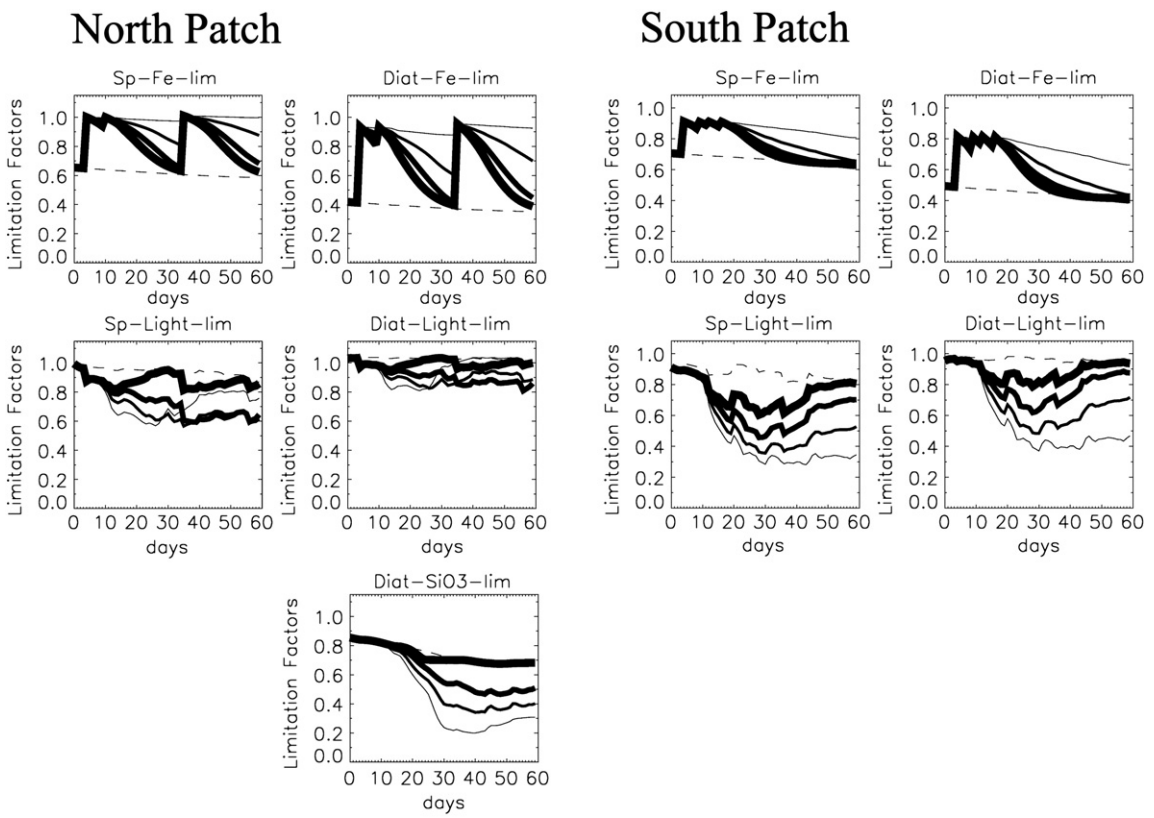

Fig. 7. Mixed layer depth averages of the growth-limitation-factors (y-axis, factors multiplied by the maximum growth rate to give relative reduction in growth rate) for the small phytoplankton (Fe and light) and for the diatoms (Fe, Si, and light) at each patch site. Lines with increasing thickness depict the simulations with no dilution, 0.5 * Coale et al. (2004) dilution, Coale et al. (2004) dilution, and 1.5 * Coale et al. (2004) dilution, respectively. Dashed line depicts the simulated unfertilized surface waters.

observations for DOC were unavailable for comparison. The difference in observed dissolved inorganic carbon (DIC) concentrations between the inside and outside patches was 15±2 mmol C/m^3 on day 28 and 16± 6 mmol C/m^3 on day 30 at the North and South Patch respectively (Table 1, Coale et al., 2004). These compared

Table 2
Simulated depth integrated (0–150 m) carbon budgets for outside and inside the iron fertilized South Patch as well as for the iron fertilized dilution and wind speed/mixed layer sensitivity experiments. Column 2 and 3 give the mean MLD (m) and the associated wind speeds (m/s)

South Patch	Mean MLD	Wind speed	Primary prod	DOC	POC prod	Loss terms	Sinking POC	Exp1	Exp 2	Total POC
Outside patch	33	10	1990	671	262	1214	119	0.07	0.08	167
No dilution	33	10	7761	1363	3337	2790	1212	0.16	0.15	595
In/Coale et al. (2004) dilution	33	10	5614	1115	1310	2150	516	0.10	0.12	309
0.5 * Coale et al., 2004 dilution	33	10	6609	1226	2111	2441	800	0.13	0.14	436
1.5 * Coale et al. (2004) dilution	33	10	4549	1010	775	1879	317	0.07	0.11	189
Wind speed * 0.7(out)	19	7	1992	670	263	1217	157	0.11	0.13	167
Wind speed * 1.3(out)	48	13	1916	651	250	1175	151	0.11	0.13	165
Wind speed * 1.6(out)	70	16	1831	626	234	1129	144	0.10	0.12	167
Wind speed * 0.7(in)	19	7	5641	1067	1563	2070	802	0.22	0.32	268
Wind speed * 1.3(in)	48	13	4624	1081	798	2013	436	0.13	0.16	234
Wind speed * 1.6(in)	70	16	3072	895	397	1591	231	0.09	0.13	172

Columns 4, 5, 6, 7 and 8 give the cumulative (day 0–60) depth integrated primary production, semi-labile DOC production, net POC production, phytoplankton mortality and grazing loss and the net sinking POC export at the depth of 150 m (all in mmol C/m2). Columns 9 and 10 summarize the mean export ratios calculated at 50 m (Sinking POC export /primary production) for days 1 to 30 and from days 31 to 60 of the simulations respectively. Column 11 gives the total water column POC inventory (mmol C/m2) on the last day (60th day) of the simulations.

well with those obtained in our simulations (11 mmol C/m^3 and 23 mmol C/m^3 at the North and South Patch, respectively). This implies that our model partitions too much of the net community production into sinking particle export and not enough carbon into the semi-labile DOC pool. Comparisons between observations on day 28 (North Patch) and day 30 (South Patch) with those obtained from same days of simulations (Table 1) were also reasonable except for the silica drawdown and biogenic silica accumulation at the simulated North Patch. The simulated TCO_2 values in the table were obtained by calculating the mean depletion (difference between unfertilized and fertilized waters) over the mixed layer depth.

Model phytoplankton growth rates depend on ambient temperature. A temperature function is used to modify the growth rates. These "temperature-specific" maximum growth rates are then multiplied by the light and nutrient limitation terms (Moore et al., 2002). The most limiting nutrient is determined from the nutrient with the lowest concentration relative to the uptake half-saturation constant. Small phytoplankton growth can be limited by N, P, Fe and light and diatom growth by N, P, Fe, Si and light. The light and nutrient terms are multiplicative allowing for co-limitation (Moore et al., 2002, 2004).

At both sites, simulated diatom and small phytoplankton growth were iron-limited for the unfertilized control throughout the simulations (Fig. 4). In the fertilized patches at both sites, the iron infusions initially relieved iron stress; as the blooms progressed, both small phytoplankton and diatoms reverted to iron-stressed

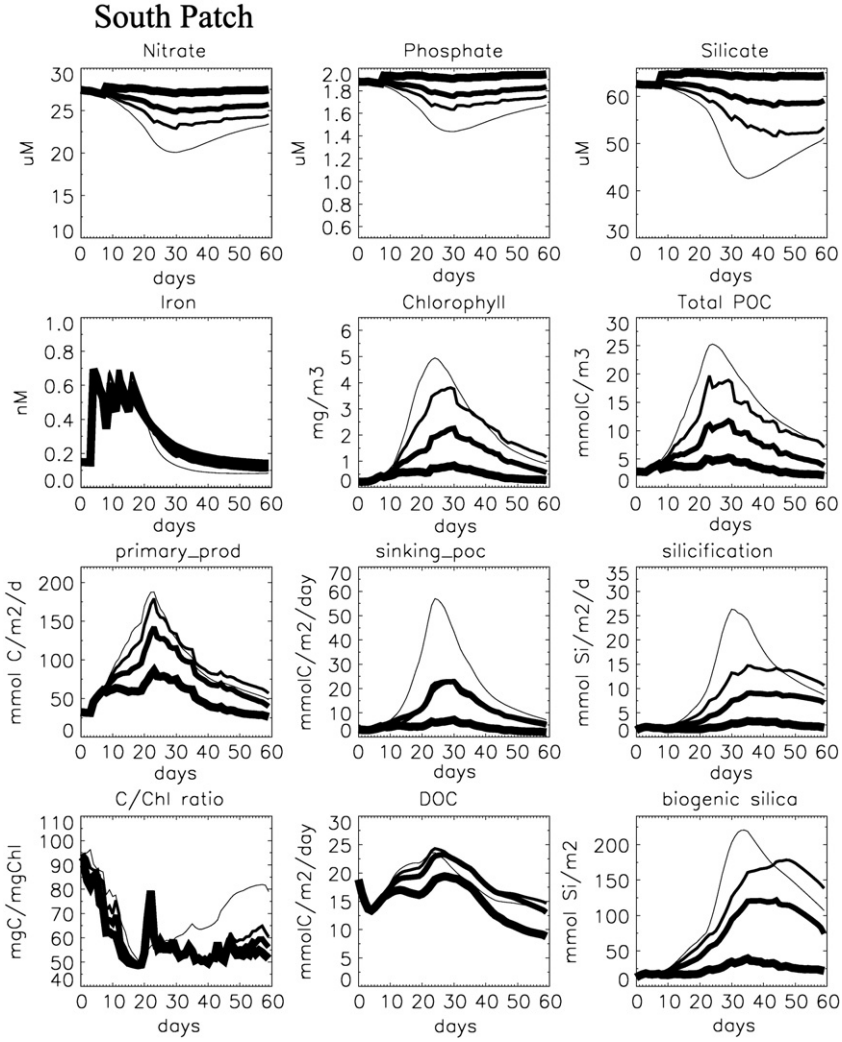

Fig. 8. Results obtained from simulations for the iron fertilized South Patch with varying wind speeds and mixed layer depths (Table 2, column 2). Lines with increasing thickness depict the simulated runs with NCEP wind forcing multiplied by 0.7, 1, 1.3 and 1.6.

conditions. At the North Patch (Fig. 4) diatoms were iron and silicon limited to about the same degree close to the end of the simulations. The observations indicate a mixed community of several species (>5 μm diameter) at the North Patch (Buesseler et al., 2005), whereas in the model, diatoms dominated the bloom, leading to stronger depletion of silica and macronutrients than in the observations. In our simulations, light limitation in unfertilized waters was minimal at both sites such that light limitation reduced maximum growth rate by ~10% at both sites. At the fertilized North Patch, light limitation played a significant role in the bloom development, reducing small phytoplankton growth rates by almost 40% and diatom growth rates by about 20% at the end of the bloom. Thus, self-shading was significant as the bloom developed. In the fertilized South Patch (Fig. 4), at peak bloom, light limitation reduced the small phytoplankton and diatom growth rates by 60% and 40% respectively. This light-limitation decreased as the bloom declined. Nutrients not depicted in Fig. 4 were never growth limiting.

Diatoms dominated the bloom at the North and South Patches in the model. In the field experiment as described in the previous paragraph the community structure at the North Patch consisted of a mixture of phytoplankton (>5 μm diameter) which included diatoms (Buesseler et al., 2005) but the diatoms never dominated the bloom. The South Patch bloom was diatom-dominated (Coale et al., 2004). In part because of the way grazing is parameterized, it is difficult for the BEC to have a mixed bloom (both small phytoplankton and diatoms). The tendency is for either small phytoplankton or diatoms to

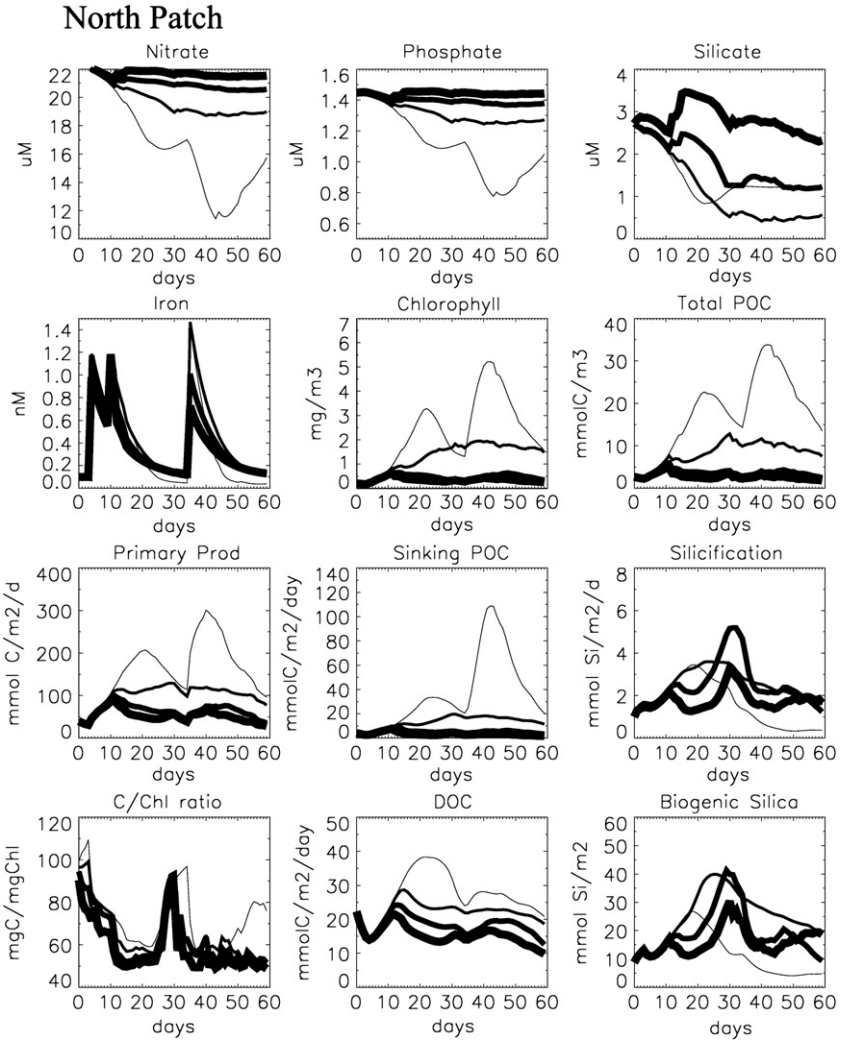

Fig. 9. Results obtained from simulations for the iron fertilized North Patch with varying wind speeds and mixed layer depths (Table 3, column 2). Lines with increasing thickness depict the simulated runs with NCEP wind forcing multiplied by 0.7, 1, 1.3 and 1.6.

bloom. This leads to the model bias at the North Patch simulations with strong diatom dominance of the bloom. We acknowledge this flaw in the model and hope to address it in future work. Despite the inherent biases in the model, the simulations were to a large extent able to recreate the prominent biogeochemical dynamics of the fertilized and unfertilized surface waters at the North and South Patches during the SOFeX. As a next step, the following two sections summarize the effects of dilution and varying mixed layer depths on bloom development.

3.2. Effects of patch dilution

Dilution acts to reduce elevated phytoplankton biomass, lower iron concentrations, and mix in macronutrients from outside the iron fertilized patches. The response of a case with no dilution would be indicative of the response to large-scale fertilization. In the dilution sensitivity plots (Figs. 5–7), the line thickness increases from the no dilution case through 0.5, 1.0 and 1.5 times the Coale et al. (2004) dilution estimates, and dashed lines represent the unfertilized surface waters. Peak bloom magnitude at each site was inversely correlated with dilution rate. At the highest dilution rate, the North Patch and South Patch blooms were depressed (max. Chl. at North Patch <1 mg/m^3; max. Chl. at South Patch <3 mg/m^3) but they were still higher than that in the unfertilized surface waters. Peak blooms at the South Patch for the different dilution rates occur at similar times but the magnitude during bloom termination were higher under lower dilution rates (Fig. 5). The macronutrient drawdown was stronger than in our standard simulations, particularly in the no dilution case. At the North Patch (Fig. 6), intermediate dilution rates resulted in an extended bloom, relative to the high and no dilution cases.

In all of the dilution cases (Fig. 7), phytoplankton iron limitation eased initially after the iron infusions but redeveloped as the bloom progressed, with the limitation increasing sooner with higher dilution rates (as iron was lost laterally from the patch). For the two highest dilution cases (1.0 and 1.5 times Coale et al.'s (2004)

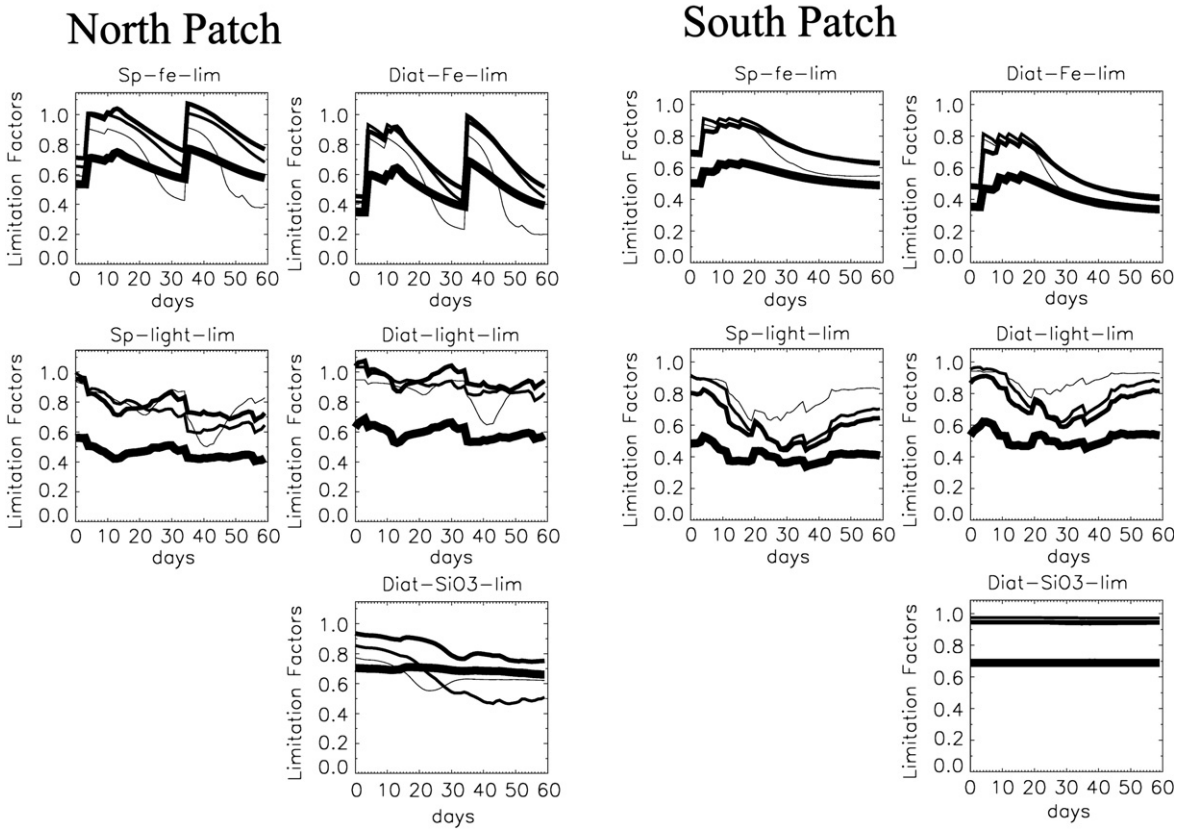

Fig. 10. Mixed layer depth averages of the growth-limitation-factors (y-axis, factors multiplied by the maximum growth rate to give relative reduction in growth rate) for the small phytoplankton (Fe and light) and for the diatoms (Fe, Si, and light) at each patch site. Lines with increasing thickness depict the simulations with NCEP wind forcing multiplied by 0.7, 1, 1.3 and 1.6.

estimates), post-bloom iron limitation levels approached that of the unfertilized control cases. Light limitation exhibited the opposite pattern increasing right after the iron injections and then easing following the bloom, though with considerably more short-term variability due to MLD fluctuations. The large range in the magnitudes of the South Patch bloom led to a corresponding large variation in the degree to which small phytoplankton and diatom growth were limited by light (Fig. 7). Higher chlorophyll concentrations increased light limitation due to self-shading of the blooms. Increasing diatom Si limitation occurred as dilution rate was lowered at the North Patch, and silicon limitation replaced iron limitation as the major nutrient factor governing diatom growth at the lower dilution rates. In effect, the amount of iron added by the injections exceeded the amount of available $Si(OH)_4$ at the community Si/Fe uptake ratio without some external Si source via lateral mixing. This pattern was also observed in the field data by Hiscock and Millero, (2005). Nutrients not depicted in Fig. 7 were never growth limiting.

3.3. Effects of changing mixed layer depths

Mixed layer depths shoal under reduced wind speeds and deepen under greater wind speeds (Tables 1 and 2). In the MLD sensitivity plots (Figs. 8–10), the line thickness increases from the 0.7, 1.0, 1.3 and 1.6 times the baseline adjusted NCEP wind forcing. Maximum bloom conditions were observed for the simulation with the shallowest MLD at both patches. The bloom at the South Patch exhibited a uniform trend such that it decreased with increased MLD. The nutrient uptake reflected this such that there was very little drawdown for the simulations with deeper mixed layers (Fig. 8). At the North Patch there were two peaks in the bloom corresponding to lowest wind speed forcing (Fig. 9, see chlorophyll and silicate drawdown). The second bloom corresponded to an increase in the silicate concentration around day 30 of the simulations, indicating a shift from a diatom to a small phytoplankton dominated bloom. This change in phytoplankton community resulted in an increase in sinking POC (Fig. 9, panel 8). The blooms for deeper mixed layer simulations at the North Patch (Fig. 9, panel 5) were muted (max. Chl. ~1 to 2 mg/m^3) despite considerable nutrient drawdown, especially silicate.

Simulated small phytoplankton and diatom iron limitation curves were not sensitive to wind speed and mixed layer depth except at the shallowest MLD case, where extreme iron limitation was observed in North Patch simulation following the large blooms (Fig. 10). Deepening the MLD affects the phytoplankton light limitation levels directly by decreasing the average light level over the deeper mixed depth because of the exponential light attenuation curve and indirectly by reducing the size of the bloom and the plankton self-shading. The depth attenuation term dominated, and light limitation was inversely related to wind speed and mixing. At the North Patch, the strongest silicon limitation occurred for low and intermediate MLD levels, though Si limitation did not replace Fe limitation as the dominant nutrient term except for the baseline NCEP forcing case, where diatom growth was reduced due to Si limitation by almost 60% between days 40 to 50. At the South Patch, small phytoplankton and diatoms maximum growth rates were reduced due to light limitation by ~40% and ~20% for the shallowest MLD

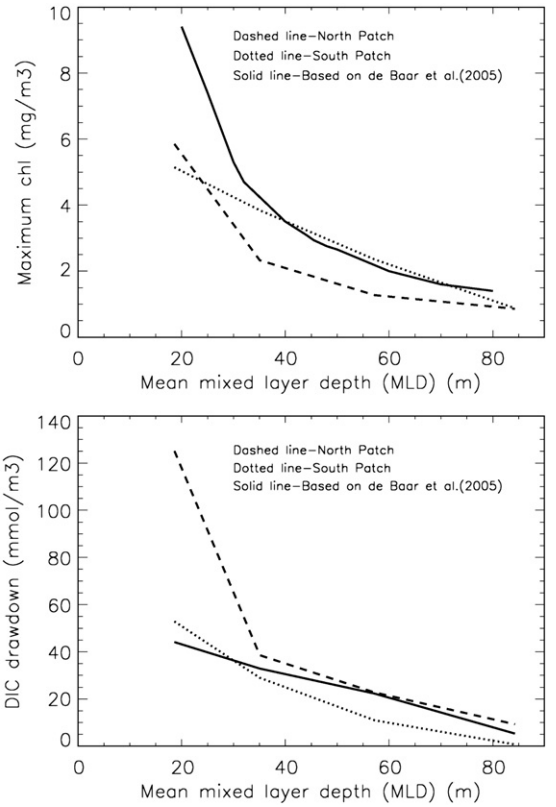

Fig. 11. Variations in simulated maximum chlorophyll (top panel) and dissolved inorganic carbon (DIC) drawdown (bottom panel) plotted against mixed layer depth (MLD) from the wind speed sensitivity experiments. DIC drawdown is defined as the initial surface DIC concentration minus the minimum surface DIC concentration over the 60 day model simulations. Dashed and dotted lines represent the North and South Patch data from varying MLD simulations and solid line is based on the trend line from Fig. 12 of de Baar et al. (2005).

Table 3
North Patch carbon budgets (refer Table 2 for details)

North Patch	Mean MLD	Wind speed	Primary prod	DOC	POC prod	Loss terms	Sinking POC	Exp1	Exp2	Total POC
Outside patch	35	11	2088	704	264	1286	151	0.11	0.12	159
No dilution	35	11	5230	1489	1108	2714	551	0.17	0.30	244
In/Coale et al. (2004) dilution	35	11	6080	1335	981	2446	486	0.11	0.10	357
0.5 * Coale et al. (2004) dilution	35	11	6018	1437	1180	2649	578	0.14	0.16	350
1.5 * Coale et al. (2004) dilution	35	11	4384	894	855	2107	234	0.10	0.14	163
Wind speed * 0.7 (out)	19	8	2133	714	273	1311	155	0.11	0.12	160
Wind speed * 1.3 (out)	57	15	1985	677	246	1230	145	0.10	0.11	157
Wind speed * 1.6 (out)	84	18	1891	647	225	1175	138	0.09	0.09	168
Wind speed * 0.7 (in)	19	8	9634	1635	2727	3165	1398	0.14	0.10	399
Wind speed * 1.3 (in)	57	15	3860	1108	467	1931	259	0.09	0.11	191
Wind speed * 1.6 (in)	84	18	3113	926	365	1634	214	0.08	0.10	183

simulation, with larger reductions with deeper mixed layers (Fig. 10).

In a study synthesizing eight iron fertilization experiments, de Baar et al. (2005) suggested that mixing of surface waters due to wind forcing has a strong influence on the amount of light received by phytoplankton for growth resulting in an inverse relationship between maximum observed chlorophyll under bloom conditions and mixed layer depth. We found a similar inverse relationship in our wind speed/MLD sensitivity experiments (Fig. 11). They also proposed that chlorophyll is not the most suitable measure of biomass because phytoplankton under iron replete conditions synthesizes more chlorophyll leading to lower carbon to chlorophyll ratios. Hence, they recommended using net drawdown of DIC as a gauge for net biomass, where net DIC drawdown is the difference between maximum DIC drawdown under bloom conditions relative to DIC values in the profile before iron additions. Our model results are consistent with the inverse relationship between MLD and DIC drawdown found by de Baar et al. (2005) across the various iron fertilization experiments such that the strongest blooms occurred in conditions with shallow mixed layers (Fig. 12 of de Baar et al., 2005; Fig. 11).

3.4. Simulated carbon and iron budgets

Depth-integrated, carbon budgets for all model cases at the South and North patches are presented in Tables 2 and 3, respectively. The SOFeX iron additions in the model led to an increase in net primary production (NPP) at both sites. The export ratios increased in the fertilized patch simulation relevant to ambient waters at the South Patch (Table 2, column 9 and 10, rows 1 and 3 (0.07 to 0.1 for days 1–30 and 0.08 to 0.12 for days

Table 4
Simulated depth integrated (0–150 m) iron budgets for outside and inside the iron fertilized South Patch as well as for the iron fertilized dilution and wind speed/mixed layer sensitivity experiments

South Patch	Bio uptake	Scavenging	Sinking export	Particulate iron	Iron added	Dissolved iron (day 60)	Dissolved iron (day 0–day 60)
Outside patch	9	0.7	0.01	1.0	0	28	2.4
No dilution	46	1.8	0.11	19.8	42	41	−11.0
In/Coale et al. (2004) dilution	25	0.9	0.01	5.8	42	28	2.4
0.5 * Coale et al. (2004) dilution	32	1.1	0.03	10.3	42	30	0.8
1.5 * Coale et al. (2004) dilution	20	0.8	0.01	3.3	42	28	2.4
Wind speed * 0.7 (out)	9	0.7	0.01	1.0	0	28	2.5
Wind speed * 1.3 (out)	8	0.7	0.01	1.0	0	28	2.4
Wind speed * 1.6 (out)	8	0.7	0.01	0.9	0	28	2.3
Wind speed * 0.7 (in)	24	0.9	0.01	6.5	41	28	2.5
Wind speed * 1.3 (in)	21	0.9	0.01	3.6	46	28	2.2
Wind speed * 1.6 (in)	16	0.8	0.01	1.9	52	29	1.7

Columns 2, 3 and 4 give the cumulative (days 0–60) depth integrated iron uptake by biology, amount of iron scavenged and the sinking particulate iron export of iron at 150 m, respectively (all in μmol Fe/m^2). Column 5, 7 and 8 give the depth integrated particulate iron and dissolved iron inventories on the last day of simulation and the difference in dissolved iron inventories between day 0 and day 60 (μmol Fe/m^2). Column 6 gives the amount of iron (μmol Fe/m^2) added during the iron infusions to the water column.

Table 5
North Patch iron budgets (refer Table 4 for details)

North Patch	Bio uptake	Scavenging	Sinking export	Particulate iron	Iron added	Dissolved iron (day 60)	Dissolved iron (day 0–day 60)
Outside patch	8	0.6	0.01	0.9	0	19	1.3
No dilution	31	2.0	0.01	8.1	125	73	−53.0
In/Coale et al. (2004) dilution	30	0.9	0.02	4.9	125	21	−0.8
0.5 * Coale et al. (2004) dilution	35	1.2	0.04	7.1	125	31	−11
1.5 * Coale et al. (2004) dilution	18	0.7	0.01	2.2	125	19	0.8
Wind speed * 0.7 (out)	8	0.7	0.01	0.9	0	19	1.4
Wind speed * 1.3 (out)	8	0.6	0.01	0.8	0	19	1.3
Wind speed * 1.6 (out)	8	0.6	0.01	0.8	0	19	1.4
Wind speed * 0.7 (in)	47	1.0	0.04	13.8	126	20	0
Wind speed * 1.3 (in)	20	0.8	0.01	2.4	125	22	−1.7
Wind speed * 1.6 (in)	17	0.8	0.01	1.9	127	22	−1.8

31–60)). At the North Patch, iron additions did not increase export ratios between days 1 to 30 (Table 3, column 9, rows 1 and 3 (0.11 in both simulations)). Export ratios decreased slightly in the iron fertilized case between days 31 to 60 (Table 3, column 10, rows 1 and 3 (0.12 to 0.1)) Buesseler et al. (2005) observed a decrease in export ratios, suggesting that possibly the diatom-dominated bloom is more buoyant under reduced iron stress. Higher export ratios at the simulated South Patch were due to higher sinking POC export associated with the elevated diatom production.

Simulated export flux decreased with increasing dilution rate and mixed layer depth in both the iron fertilized patches. In the case of dilution, loss of iron due to lateral mixing out of the patch prevented phytoplankton growth, resulting in decreased export. Similarly, higher wind speeds reduced primary production and sinking POC export due to elevated light limitation within the deeper mixed layers. At the fertilized North Patch, the simulation with the deepest mixed layer depth had a marginal increase in export ratio from days 31 to 60 due to the second bloom (Table 3, column 10; Fig. 9).

Depth and time-integrated iron budgets for all of the model cases are presented in Tables 4 and 5. Comparing the base fertilized and unfertilized simulations, the percentage of added iron that was taken up by biology (Tables 4 and 5, column 2), and sinking particulate iron export (Tables 4 and 5, column 4) were similar at both the North and South Patches. The percentage of added iron that was lost to scavenging (Tables 4 and 5, column 3) were also similar at both patches. Iron scavenging rate is parameterized based on a non-linear function of the model iron concentration, a higher concentration leads to higher scavenging rates. The iron budgets for a shorter duration (example, 5 days) immediately following iron infusions at both the North and South Patches suggested a higher percentage of iron being scavenged compared to that going to biological uptake and export. This was due to an increase in model iron concentration following iron additions.

Iron budgets for the sensitivity studies with varying dilution scenarios at the both the fertilized north and south sites demonstrate a decrease in iron uptake by biology with increased dilution. This was because dilution aided the loss of iron from the patch, making less iron available for phytoplankton. In reality much of the laterally exported iron would be consumed by phytoplankton, just not in the core of the fertilized patch. The dissolved iron concentration at the end of simulations (Tables 4 and 5, column 7) was highest for the no dilution case at both North and South Patches. The sensitivity studies with modified mixed layer depths resulted in increased iron uptake at both the fertilized patches at shallower MLD.

4. Summary and discussion

Our 1-D coupled biological–physical simulations reproduce the SOFeX observations to a large extent with a few caveats discussed below. The iron-fertilized bloom in our simulations was dominated by diatoms at both the patches, resulting in excessive silicate drawdown in the North Patch. The simulated sinking POC fluxes were also higher than those observed during the SOFeX experiment, in part due to the diatom dominance at the North Patch. Another reason for this could be that the model was partitioning too much carbon into sinking POC rather than DOC. de la Rocha (2003) suggested that the reduction in carbon export out of the euphotic zone during natural blooms could be due to increased flow of carbon through the microbial loop by microzooplankton and bacteria resulting in the regeneration of CO_2 and nutrients within the euphotic zone. Boyd et al. (2000) and Strass (2002) found that there was an increase in

microzooplankton and bacteria biomass after mesoscale iron-addition experiments such that some carbon fixed after iron addition was routed into the microbial loop and DOC pool instead of being exported to deeper waters. DOC observations were not available to directly address this possibility. The export estimates of Buesseler et al. (2005) in conjunction with the production estimates from Lance et al. (2007) imply very low export ratios for the diatom-dominated bloom at the South Patch. Export ratios varied from 0.06 to 0.11 during the first 3 weeks after the first iron fertilization (Buesseler et al., 2005). High-latitude diatom blooms often have much higher export efficiencies (Buesseler 1998; Dunne et al., 2005). Thus, the observations may underestimate export, or the export efficiency was unusually low during SOFeX.

The mixed layer depth sensitivity experiments suggested that shallow mixed layers enhance the biological response to iron fertilization, in particular the peak chlorophyll bloom magnitude. The results of our sensitivity study varying MLD were consistent with de Baar et al.'s (2005) study across different fertilization experiments. In our simulations, the maximum chlorophyll yield at the lowest mixed layer depth was limited by the quadratic phytoplankton aggregation losses which become significant under bloom conditions. The DIC drawdown values obtained from our simulations were within the range of observations used by de Baar et al. (2005). In their study, de Baar et al. (2005) compared iron fertilization experiments that were done at different regional as well as seasonal conditions that include different wind forcings, ambient temperatures, macronutrients, ocean biology and light climate. These experiments also differed in the lengths of field campaign and hence, the available observational data also varied. The amounts of iron added during each of these iron fertilization experiments were also different. The trend line based on their study, hence, incorporates these wide differences in its estimates of the relationship between mixed layer depth and maximum chlorophyll and DIC drawdown. Given that we compare these relationships at a particular region, the plots match reasonably well. Our results in conjunction with the SOFeX field observations and the de Baar et al. (2005) synthesis suggest that blooms in the Southern Ocean will tend to become light-limited or iron-light co-limited in most cases, except when mixed layer depths are quite shallow. This self-shading effect may explain the persistence of the SOIREE bloom, which was still apparent in satellite data almost 40 days after the initial fertilization (Boyd and Law, 2001). Reduced growth rates due to self-shading slow the depletion of nutrients allowing high biomass to persist for a longer period of time. These lowered growth rates are still sufficient to offset losses to grazing and other processes. Fitch and Moore (2007) recently found an inverse correlation between bloom occurrence and wind speed in the Southern Ocean marginal ice zone.

At the North Patch the simulations both outside and inside the iron fertilized patches clearly indicated co-limitation by light, iron and silicate. The South Patch was, however, only limited by iron and light as silicate concentrations are higher south of the ACC. The sensitivity experiments with different dilution rates suggested that increasing dilution at the North Patch reduced the silicate limitation due to addition of silicate from surrounding waters into the patch, consistent with field observations (Hiscock and Millero, 2005). At the North Patch, the diatom response involves a trade-off between iron loss and silicate gain via lateral mixing. The South Patch no dilution simulation had a maximum nutrient drawdown, resulting in higher net primary productivity and chlorophyll peak, because the iron remained within patch and macronutrients were not depleted.

Deliberate iron enrichment increases the total DIC loss from surface waters such that the ratio between net DIC losses to amount of iron added via enrichment can be used as a measure for the efficiency of DIC removal from surface waters. These were estimated by de Baar et al. (2005) for eight mesoscale iron fertilization experiments done so far. Dilution of the patch is an uncertainty that prevents accurate measurements of net DIC losses as the observed DIC drawdown does not equal the actual net community production (de Baar et al., 2005). Hence, only approximate estimates of net DIC loss during iron fertilization experiments can be made. The amount of iron taken up by phytoplankton is not accurately known as scavenging and other losses during the experiment prevent complete uptake of added iron. The DIC/Fe efficiency estimated by de Baar et al. (2005) was based on the average DIC removal over the mixed layer and the total amount of iron added during the experiment. The ratio was 4624 (mol C/mol Fe) and 7330 (mol C/mol Fe) on day 39 and day 20 at the fertilized North and South Patch respectively during the SOFeX. The DIC/Fe efficiency from our simulations on the same days were 8697 (mol C/mol Fe) and 7200 (mol C/mol Fe) at the fertilized North and South Patch respectively. The close agreement between this DIC/Fe ratio in our South Patch simulation and the observations, again suggests the model is removing the correct amount of DIC, but perhaps portioning too much of this into sinking POC and not enough into DOC. The simulated diatom dominated bloom resulted in the higher DIC/Fe efficiencies at the North Patch. The DIC/

Fe efficiencies for the six other mesoscale iron fertilization experiments were between 1668 (mol C/mol Fe) to 16887 (mol C/mol Fe) (de Baar et al., 2005).

SOFeX was designed such that the observing period of fertilized waters was longer than in previous in situ iron fertilization studies. Observations of the South Patch captured almost the complete cycle of bloom formation and termination, with the tail end of the bloom shortly after the completion of the field observations. But at the North Patch, the bloom appears to have persisted for a longer period. Our simulation results indicate that the North Patch bloom continued to be significant even on the 60th day of the simulation. Shipboard observations ended on day ~45 of our simulations. Continuing profiling float measurements also suggested relatively higher export at day ~55 (Bishop et al., 2004). Field campaigns for a longer period, though difficult logistically could be useful to estimate the prolonged affects of dilution, which results in increased mixing and supply of macronutrients from unfertilized waters. Future iron fertilization experiments could also be performed over a larger region as this would minimize the effects of dilution. Alternatively, natural iron sources such as the Kerguelen Islands (Blain et al., 2001; Bucciarelli et al., 2001) can also be used to study iron fertilization where distance from the iron source is a proxy for time since iron addition. These more steady state systems would eliminate the logistical problems presented by an extended Southern Ocean patch field experiment of several months.

Acknowledgments

We would like to thank the crew and all support personnel on the *R/V* Revelle, the Melville, and the Polar Star and all the investigators of the SOFeX project. Thanks to Kenneth Coale, Ken Johnson, Ken Buesseler, Jodi Brewster, Veronica Lance, William T. Hiscock, Mark Altabet and Craig Hunter for generously sharing their data during the course of this work. This work was supported by NASA grant NAG5-12520 from the NASA Ocean Biogeochemistry Program.

References

Abbott, M.R., Richman, J.G., Letelier, R.M., Bartlett, J.S., 2000. The spring bloom in the Antarctic Polar Frontal Zone as observed from a mesoscale array of bio-optical sensors. Deep-Sea Res., Part II 47 (707), 3285–3314.

Abraham, E.R., Law, C.S., Boyd, P.W., Lavender, S.J., Maldonado, M.T., Bowie, A.R., 2000. Importance of stirring in the development of an iron-fertilized phytoplankton bloom. Nature 407 (6805), 727–730.

Bishop, J.K.B., Wood, T.J., Davis, R.E., Sherman, J.T., 2004. Robotic observations of enhanced carbon biomass and export at 55°S during SOFeX. Science 304 (5669), 417–420.

Blain, S., Treguer, P., Belviso, S., Bucciarelli, E., Denis, M., Desabre, S., Fiala, M., Martin, J.V., Le Fevre, J., Mayzaud, P., Marty, J.C., Razouls, S., 2001. A biogeochemical study of the island mass effect in the context of the iron hypothesis: Kerguelen Islands, Southern Ocean. Deep-Sea Res., Part I 48 (1), 163–187.

Boyd, P.W., 2002. Environmental factors controlling phytoplankton processes in the Southern Ocean. J. Phycol. 38, 844–861.

Boyd, P.W., Law, C.S., 2001. The Southern Ocean Iron Release Experiment (SOIREE)—introduction and summary. Deep-Sea Res., Part 2, Top. Stud. Oceanogr. 48 (11–12), 2425–2438.

Boyd, P.W., LaRoche, J., Gall, M., Frew, R., McKay, R.M.L., 1999. Role of iron, light, and silicate in controlling algal biomass in subantarctic waters SE of New Zealand. J. Geophys. Res. 104 (C6), 13395–13408.

Boyd, P.W., Watson, A.J., Law, C.S., Abraham, E.R., Trull, T., Murdoch, R., Bakker, D.C., Bowie, A.R., Buesseler, K.O., Chang, H., Charette, M., Croot, P., Downing, K., Frew, R., Gall, M., Hadfield, M., Hall, J., Harvey, M., Jameson, G., LaRoche, J., Liddicoat, M., Ling, R., Maldonado, M.T., McKay, R.M., Nodder, S., Pickmere, S., Pridmore, R., Rintoul, S., Safi, K., Sutton, P., Strzepek, R., Tanneberger, K., Turner, S., Waite, A., Zeldis, J., 2000. A mesoscale phytoplankton bloom in the polar Southern Ocean stimulated by iron fertilization. Nature 407, 695–702.

Brown, S.L., Landry, M.R., 2001. Mesoscale variability in biological community structure and biomass in the Antarctic Polar Front region at 170 W during austral spring 1997. J. Geophys. Res. 106, 13917–13930.

Brzezinski, M.A., Jones, J.L., Demarest, M.S., 2005. Control of silica production by iron and silicic acid during the Southern Ocean Iron Experiment (SOFeX). Limnol. Oceanogr. 50 (3), 810–824.

Buesseler, K.O., 1998. The decoupling of production and particulate export in the surface ocean. Glob. Biogeochem. Cycles 12 (2), 297–310.

Buesseler, K.O., Andrews, J.E., Pike, S., Charette, M.A., Goldson, L.E., Brzezinski, M.A., Lance, V.P., 2005. Particle export during the Southern Ocean Iron Experiment (SOFeX). Limnol. Oceanogr. 50 (1), 311–327.

Bucciarelli, E., Blain, S., Treguer, P., 2001. Iron and manganese in the wake of the Kerguelen Islands (Southern Ocean). Mar. Chem. 73 (1), 21–36.

Campbell, J.W., Aarup, T., 1989. Photosynthetically available radiation at high-latitudes. Limnol. Oceanogr. 34 (8), 1490–1499.

Coale, K.H., Johnson, K.S., Chavez, F.P., Buesseler, K.O., Barber, R.T., Brzezinski, M.A., Cochlan, W.P., Millero, F.J., Falkowski, P.G., Bauer, J.E., Wanninkhof, R.H., Kudela, R.M., Altabet, M.A., Hales, B.E., Takahashi, T., Landry, M.R., Bidigare, R.R., Wang, X., Chase, Z., Strutton, P.G., Friederich, G.E., Gorbunov, M.Y., Lance, V.P., Hilting, A.K., Hiscock, M.R., Demarest, M., Hiscock, W.T., Sullivan, K.F., Tanner, S.J., Gordon, R.M., Hunter, C.N., Elrod, V.A., Fitzwater, S.E., Jones, J.L., Tozzi, S., Koblizek, M., Roberts, A.E., Herndon, J., Brewster, J., Ladizinsky, N., Smith, G., Cooper, D., Timothy, D., Brown, S.L., Selph, K.E., Sheridan, C.C., Twining, B.S., Johnson, Z.I., 2004. Southern ocean iron enrichment experiment: carbon cycling in high-and low-Si waters. Science 304, 408–414.

de Baar, H.J., Boyd, P.W., Coale, K.H., Landry, M.R., Tsuda, A., Assmy, P., Dorothee, C.E.B., Bozec, Y., Barber, R.T., Brzezinski, M.A., Buesseler, K.O., Boye, M., Croot, P.L., Gervais, F., Gorbunov, M.Y., Harrison, P.J., Hiscock, W.T., Laan, P., Lancelot, C., Law, C.S., Levasseur, M., Marchetti, A., Millero, F.J.,

Nishioka, J., Nojiri, Y., van Oijen, T., Riebesell, U., Micha, J.A.R., Saito, H., Takeda, S., Timmermans, K.R., Marcel, J.W.V., Waite, A.M., Wong, C.S., 2005. Synthesis of iron fertilization experiments: from the iron age in the age of enlightenment. J. Geophys. Res. 110, C09S16. doi:10.1029/2004JC002601.

Dehairs, F., Lancelot, C., André, L., Frankignoulle, M., Deleersnijder, E., Becquevort, S., Cardinal, D., Cattaldo, T., Delille, B., Elskens, M., Fagel, N., Goosse, H., Hannon, E., Navez, J., Probst, G., Schoemann, V., Kopczynska, E., Kostianoy, A., 2000. An Integrated Approach to Assess Carbon Dynamics in the Southern Ocean, Final Scientific Report, A4/DD/B11 — B14. available at www.co2.ulg.ac.be/objects/Belcanto_Final_Report.pdf.

de la Rocha, C.L., 2003. The biological pump. In: Holland, H.D., Turekian, K.K. (Eds.), Treatise on Geochemistry. Pergamon, Oxford, pp. 83–111.

Doney, S.C., 1996. A synoptic atmospheric surface forcing data set and physical upper ocean model for the U.S. JGOFS Bermuda Atlantic Time-Series Study (BATS) site. J. Geophys. Res., Oceans 101, 25,615–25,634.

Dunne, J.P., Armstrong, R.A., Gnanadesikan, A., Sarmiento, J.L., 2005. Empirical and mechanistic models for the particle export ratio. Glob. Biogeochem. Cycles. doi:10.1029/2004GB002390.

Fennel, K., Abbott, M.R., Spitz, Y.R., Richman, J.G., Nelson, D.M., 2003. Modeling controls of phytoplankton production in the southwest Pacific sector of the Southern Ocean. Deep-Sea Res., Part 2, Top. Stud. Oceanogr. 50 (3–4), 769–798.

Fitch, D.T., Moore, J.K., 2007. Wind speed influence on phytoplankton bloom dynamics in the Southern Ocean Marginal Ice Zone. J. Geophys. Res. 112, C08006. doi:10.1029/2006JC004061.

Geider, R.J., MacIntyre, H.L., Kana, T.M., 1998. A dynamic regulatory model of phytoplankton acclimation to light, nutrients, and temperature. Limnol. Oceanogr. 43, 679–694.

Gervais, F., Riebesell, U., Gorbunov, M.Y., 2002. Changes in primary productivity and chlorophyll a in response to iron fertilization in the Southern Polar Frontal Zone. Limnol. Oceanogr. 47, 1324–1335.

Helbling, E.W., Villafane, V.E., Holmhansen, O., 1995. Variability of phytoplankton distribution and primary production around Elephant Island, Antarctica, during 1990–1993. Polar Biol. 15 (4), 233–246.

Hiscock, M.R., The regulation of primary productivity in the Southern Ocean, 2004. PhD thesis, Nicholas School of the Environment and Earth Sciences, Duke University.

Hiscock, W.T., Millero, F.J., 2005. Nutrient and carbon parameters during the SOFeX. Deep-Sea Res. I 52, 2086–2108.

Kalnay, E., Kanamitsu, M., Kistler, R., Collins, W., Deaven, D., Gandin, L., Iredell, M., Saha, S., White, G., Woollen, J., Zhu, Y., Chelliah, M., Ebisuzaki, W., Higgins, W., Janowiak, J., Mo, K.C., Ropelewski, C., Leetmaa, A., Reynolds, R., Jenne, R., 1996. The NCEP/NCAR reanalysis project. Bull. Am. Meteorol. Soc. 77, 437–471.

Lance, V.P., Hiscock, M.R., Hilting, A.K., Stuebe, D.A., Bidigare, R.R., Smith Jr., W.O., Barber, R.T., 2007. Primary productivity, differential size fraction and pigment composition responses in two Southern Ocean in situ iron enrichments. Deep-Sea Res. I 54 (5), 747–773. doi:10.1016/j.dsr.2007.02.008.

Large, W.G., McWilliams, J.C., Doney, S.C., 1994. Oceanic vertical mixing: a review and a model with a non-local boundary layer parameterization. Rev. Geophys. 32, 363–403.

Luo, C., Mahowald, N., del Corral, J., 2003. Sensitivity study of meteorological parameters on mineral aerosol mobilization, transport and distribution. J. Geophys. Res. 108 (D15), 4447. doi:10.1029/2003JD0003483.

Martin, J.H., 1990. Glacial-interglacial CO2 change: the iron hypothesis. Paleoceanography 5, 1–13.

McClain, C.R., Cleave, M.L., Feldman, G.C., Gregg, W.W., Hooker, S.B., Kuring, N., 1998. Science quality SeaWiFS data for global biosphere research. Sea Technology September, 10–16.

McClain, C.R., Feldman, G.C., Hooker, S.B., 2004. An overview of the SeaWiFS project and strategies for producing a climate research quality global ocean bio-optical time series. Deep Sea Res., Part II 51, 5–42.

Mitchell, B.G., Brody, E.A., Holm-Hansen, O., McClain, C., Bishop, J., 1991. Light limitation of phytoplankton growth in Antarctic waters. Glob. Biogeochem. Cycles 4, 5–12.

Moore, J.K., Doney, S.C., 2006. Remote sensing observations of ocean physical and biological properties in the region of the Southern Ocean Iron Experiment (SOFeX). J. Geophys. Res 111, C06026. doi:10.1029/2005JC003289.

Moore, J.K., Doney, S.C., Kleypas, J.A., Glover, D.M., Fung, I.Y., 2002. An intermediate complexity marine ecosystem model for the global domain. Deep-Sea Res., II 49, 403–462.

Moore, J.K., Doney, S.C., Keith, L., 2004. Upper ocean ecosystem dynamics and iron cycling in a global three-dimensional model. Glob. Biogeochem. Cycles 18, GB4028. doi:10.1029/2004GB002220.

Nelson, D.M., Smith Jr., W.O., 1991. Sverdrup revisited: critical depths, maximum chlorophyll levels, and the control of southern ocean productivity by irradiance mixing regime. Limnol. Oceanogr. 36, 1650–1661.

Smetacek, V., 2001. EisenEx: international team conducts iron experiment in Southern Ocean. U.S. JGOFS News 11 (1), 11–14.

Smith, W.O., Lancelot, S., 2004. Bottom-up versus top-down control in phytoplankton of the Southern Ocean. Antarct. Sci. 16 (4), 531–539.

Strass, V.H., 2002. EisenEx-1: test of the iron hypothesis in a Southern Ocean eddy. EOS: Trans., AGU Abstracts of 2002 Ocean Sciences Meeting.

Sunda, W.G., Huntsman, S.A., 1997. Interrelated influence of iron, light and cell size on marine phytoplankton growth. Nature 390, 389–392.